



# Stability analysis of the Cold Metal Transfer (CMT) brazing process for galvanized steel plates with ZnAl<sub>4</sub> filler metal

Gustavo Henrique Truppel<sup>1,2</sup> · Matthias Angerhausen<sup>2</sup> · Alexandros Pipinikas<sup>2</sup> · Uwe Reisgen<sup>2</sup> · Luiz Eduardo dos Santos Paes<sup>1</sup>

Received: 29 January 2019 / Accepted: 4 April 2019 / Published online: 23 April 2019  
© Springer-Verlag London Ltd., part of Springer Nature 2019

## Abstract

In order to achieve lower CO<sub>2</sub> emissions and lower fuel consumption, modern motor vehicle industries have been reducing automotive weight with an increasing degree in the past years by replacing steel structures with brazed and welded components of steel and lightweight metals. In this context, the combination of galvanized steel and aluminum admits considerable application potential. Joints of the two cited different types of materials can be produced by partial brazing, through the Cold Metal Transfer (CMT) process with addition of zinc-based wire alloys. However, stability analysis for this process is still not well understood. Most papers focus on metallurgical characteristics such as intermetallic phase formation and joint strength. In order to assess stability, bead on plate samples made of ZnAl<sub>4</sub> deposits on an automotive DX56D + Z140 galvanized steel was statistically correlated to current and voltage oscillograms as well as high-speed images, after variation of the IBoost parameter from 30 to 150 A. Short-circuit and arc burning times were acquired and used to compute the Vilarinho Regularity Index for Short-Circuit Transfer (IV<sub>sc</sub>), which is based on variation coefficients. The lower the IV<sub>sc</sub>, the more stable is the metal transfer. The index was used to assess bead homogeneity. The results pointed that bead homogeneity was found only for IBoost values below 97 A. However, stability was reached for IBoost levels of 97 A (with homogeneous bead) and 150 A (without homogeneous bead). This means that to determine homogeneity, the metal transfer stability, determined through IV<sub>sc</sub>, is an indicator, but other factors such as current level and its effects over the melt pool must also be considered.

**Keywords** GMAW · Wettability · Monitoring · Boost current · Statistics

## 1 Introduction

In the automotive industry, CO<sub>2</sub> emission is a concern, while the environmental laws become stricter. In order to overcome this issue, new alternatives have been proposed, such as the manufacturing of light components with high specific strength. When aluminum alloys are preferred, the vehicle weight is significantly reduced, which contributes to lower fuel consumption. According to Unel and Taban [1], recent developments have shown that is possible to reach up to 50%

less Body-In-White (BIW) weight when steel is replaced by aluminum. In addition, for each 10% of weight reduction, fuel savings improve 7%.

However, vehicles should have steel parts, due to the mechanical strength required in some applications. As a result, there is a need for development of dissimilar joining methods.

The main challenge regards to differences in mechanical properties between materials, such as melting point and electric and thermal conductivities, besides expansion rates, which are problematic to achieve high-quality joints [2]. Galvanic corrosion can also happen because of potential difference between the plates, and when high temperatures are reached, fragile intermetallic compounds are formed in the interface. These factors may reduce the joint strength [3].

Although other joining methods as mechanical joining (i.e., bolts) and adhesive bonding are available in the market, in these cases, the specific strength is limited, and the usual geometry configuration [1]. When conventional welding processes are selected, other difficulties arise such as the presence

✉ Luiz Eduardo dos Santos Paes  
luiz.paes@posgrad.ufsc.br

<sup>1</sup> Mechanical Engineering's Department, Universidade Federal de Santa Catarina, Florianópolis, Santa Catarina, Brazil

<sup>2</sup> Institut für Schweißtechnik und Fügetechnik, Rheinisch-Westfälische Technische Hochschule Aachen, Aachen, Nordrhein-Westfalen, Germany

of spatters, porosity, inadequate bead geometry, loss of corrosive protection, and excessive hardness in the fusion zone (FZ) and in the heat-affected zone (HAZ) [4]. Solid state methods have also been tested as for example explosion welding [5], diffusion welding [6], friction welding [7], and friction stir welding [8]. Yet, these approaches have not been fully implemented in industry due to restrictions in joint size, welding position, pressured needed, and equipment cost [9–11]. Considering the cited issues, the most appropriate process in this demand is brazing [4].

Opposed to welding, where both the filler material and base material reach the melting point, in brazing, only the filler material is melted. The capillary action constitutes the dominant physical principle. Then, bead wettability is essential, and can be assessed through contact angle measurements. Contact angles below  $90^\circ$  are positive indicators of wettability [11]. Some studies have shown that the higher the bead width and the lower the contact angle, the better are the mechanical properties of the joint [12, 13].

Cao et al. [14] states that when galvanized steel is used, not only the corrosion protection is improved, but also the brazing process. The immediate zinc vaporization allows the iron to be directly exposed to the filler metal, and then contact angle around  $35^\circ$  is obtained. Without the zinc coating, the surface gets oxidized, and the material does not wet well, with contact angles around  $55^\circ$ . That is why galvanized steels are preferred when brazing is required [15–17]. However, in these applications, zinc alloys should be used, instead of copper alloys. The main reason is related to the higher melting point of copper, which is above the zinc vaporization temperature (over  $940^\circ\text{C}$ ). Even though copper shows good wettability, excessive zinc vaporization can impact on joint integrity [18].

The melted metal flow is influenced by its surface tension, viscosity, dynamic behavior, vapor pressure, gravity, physical properties, metallurgical reactions with atmosphere, and surface oxides. The bonding is caused by diffusion, which propitiates the formation of intermetallic compounds (IMCs) in the interface [11]. According to Mohammadpour et al. [19], the hardness of these IMCs can reach values of 1000 Hv.

The formation of IMC is influenced by cooling rates and thermal history [19–24]. In terms of process parameters, this means that it is influenced by the heat input. As only the filler material reaches the melting point in brazing, less heat is required to accomplish the joint when the process is compared with welding. Then, besides the reduced distortion and residual stress levels [11], the intermetallic layer can also decrease, and this fact results in good mechanical properties [2, 21, 22].

The well-known version of brazing is the oxyacetylene, but the formation of IMCs is excessive and restricts its use [10]. Another alternative was covered by Dong et al [23], who studied dissimilar brazing of aluminum to galvanized steel through the Tungsten Inert Gas (TIG) arc process, and found satisfactory values for IMCs thickness ( $2\ \mu\text{m}$ ). However, it is

important to mention that TIG usually shows low welding speeds and deposition rates, which limits productivity. The process that combines productivity and relatively low heat input simultaneously is the Metal Inert Gas Brazing (MIGB) [4].

The MIGB process is similar to the MIG welding process, but here only the filler metal melts. The physical principle is the same. A voltaic arc is formed between the electrode and the plate after current flow. Shielding gas and an energy source are also required. The application of MIGB process has grown during manufacturing of car body parts roofs to side panel and fuel tank, where more stiffness and leak proof joining are required [4]. Li et al. [10] studied the influence of torch position and angle over the resultant brazing beads with the MIGB pulsed process. In a subsequent work, Li et al. [9] improved process understanding after analyzing pulse current, base current, pulse period, and base period parameters. Basak et al. [10] investigated the effect of heat input on bead width and wetting angle for pulsed MIGB. When the heat input varied from 155 to 235 J/mm, the bead width increased from 9.4 to 12.6 mm, while the wetting angle reduced from  $61^\circ$  to  $37^\circ$ . Uniform beads were obtained with satisfactory mechanical strength. As the heat input can exert great influence over the final result, it is essential to control it. A more sophisticated version of MIG process has been widely applied for dissimilar joining and is denominated Cold Metal Transfer (CMT).

The CMT was initially developed by Fronius, in Austria, in 2004. The process operates with the short-circuit metal transfer, but with high control level. While in the conventional MIG, the droplet constriction occurs fundamentally due to electromagnetic force, in the CMT, a forward and backward wire movement assists the metal transfer [25]. This movement is executed by a servomotor, located in the torch, with a frequency up to 70 Hz. Then, the droplet is transferred smoothly, without spatters [26]. Besides that, the heat input is almost the half of that needed in conventional MIG, considering the same deposition rate [27]. It is possible to control the amount of heat delivered over the plate [24], which is essential during brazing of dissimilar materials, as mentioned before. Figure 1 illustrates schematically the wire oscillation in CMT.

The typical current and voltage CMT signals are displayed in Fig. 2. A cycle is defined as the period required for droplet transfer coming from electrode melting to the melt pool.

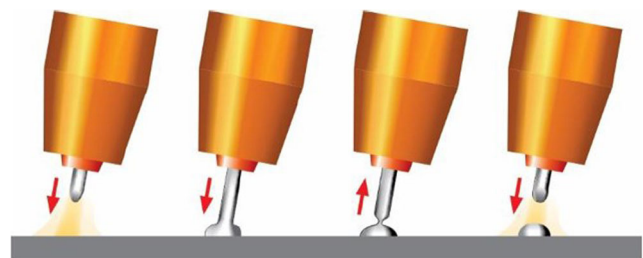
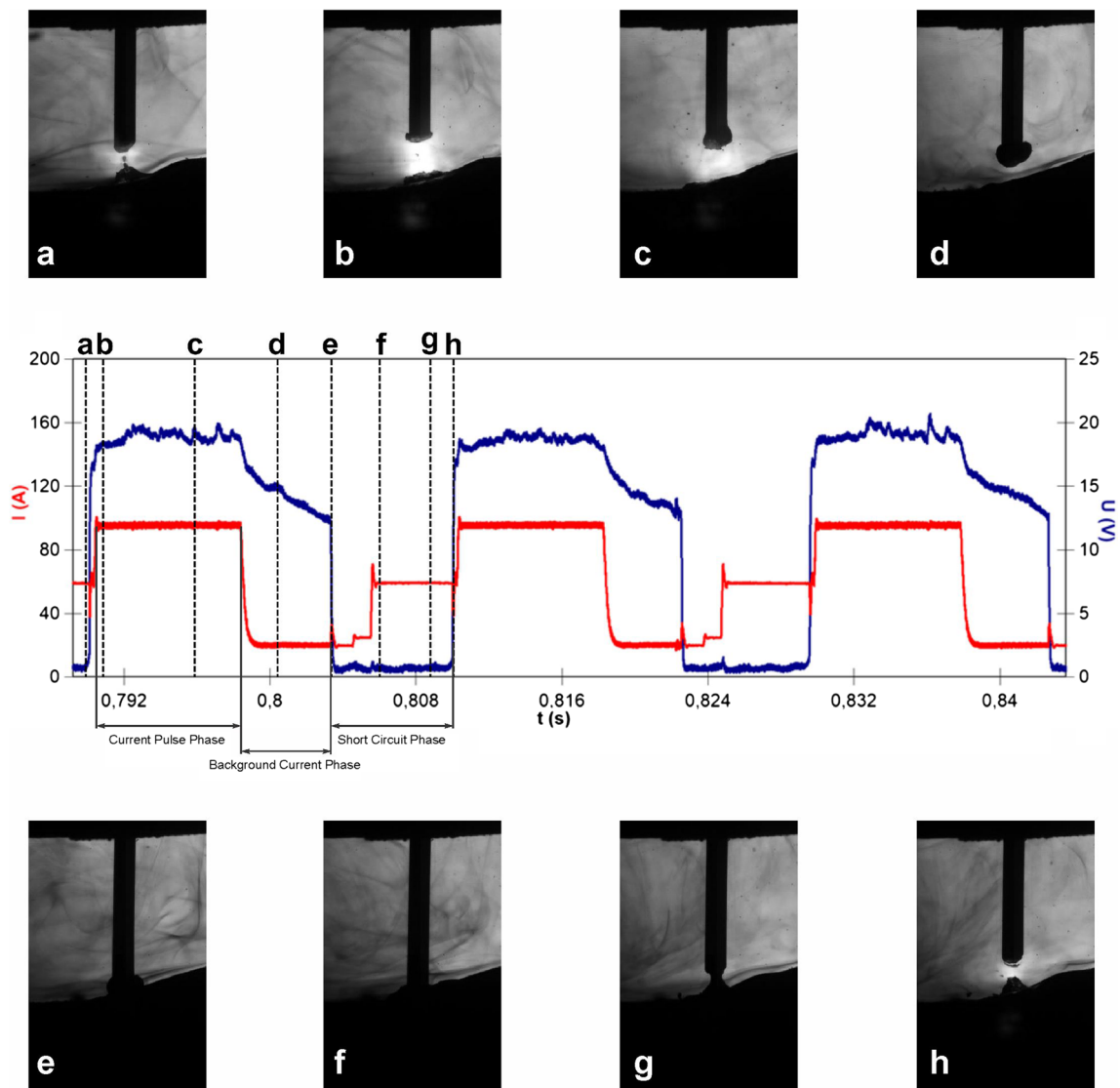


Fig. 1 Forward and backward movement for CMT process



**Fig. 2** Typical CMT oscillogram with current and voltage signals and correspondent metal transfer behavior

According to Zhang et al. [26], three phases can be distinguished:

- (i) Current pulse phase: is represented by a current pulse (IBoost) with the aim to facilitate arc ignition, promote electrode fusion, and form the metal droplet during a configured pulse time.
- (ii) Background current phase: after the droplet formation during the pulse phase, the droplet tends to grow and transfer in the globular mode, which could result in spatters. In order to avoid this, the current reduces abruptly and is kept constant until short-circuiting.
- (iii) Short-circuit phase: in this phase, the wire contacts the melt pool and the arc voltage is extinguished. Then, the servomotor coupled to the torch executes the backward wire movement, which facilitates the metal transfer. As a result of the described oscillation, the droplet is

transferred in a lower current level, and this contributes for the controlled heat input to the plate as well as for the absence of spatters.

Phases (i) and (ii) belong to arc burning time, while phase (iii), to short-circuit time. The metal transfer behavior can be analyzed based on high-speed camera. The cycle starts at point “a.” Points “b” and “c” are related to the current pulse phase. This stage is necessary for drop formation in the electrode tip. Then, the current is reduced in point “d” to limit spatter and metal vaporization before short-circuiting. Point “e” is the moment immediately before the short circuit. The metal transfer assisted by mechanical retraction can be observed in frames “f” and “g.” In this last one, a bridge is evident. Finally, the cycle ends in frame “h,” after detachment.

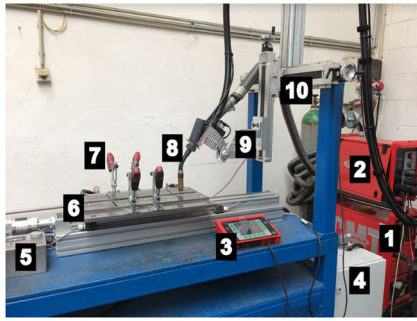


**Fig. 3** Brazing tests configuration. 1 Power source. 2 Wire feeder. 3 Interface. 4 Linear table source. 5 Linear table interface. 6 Linear table. 7 Clamping system. 8 CMT torch. 9 Torch support. 10 Shielding gas

Most works relative to CMT brazing focus on metallurgical characteristics such as intermetallic formation and its influence over the joint mechanical strength [14, 20, 22, 28–33]. Just a few ones are dedicated to process stability [30–32], which is essential for the selection of suitable parameters. Stability can be analyzed through different ways, for example, with current and voltage signal measurements in time or frequency domains [9], cyclograms, arc voltage variance, and probability distribution [10] or through captured images with high-speed cameras associated to current and voltage oscillograms [32]. Alves et al. [34] chose a criterion that quantifies metal transfer stability in short-circuit mode. This criterion is based on the premise that metal transfer is related to arc burning and short-circuit times constancy. When these periods present low dispersion, heat transfer to the plate becomes stable, as well as the bead geometry and metallurgical alterations. To study stability with this criterion, it is necessary to calculate the Vilarinho Regularity Index for Short-Circuit Transfer (IV<sub>SC</sub>), according to Eq. (1).

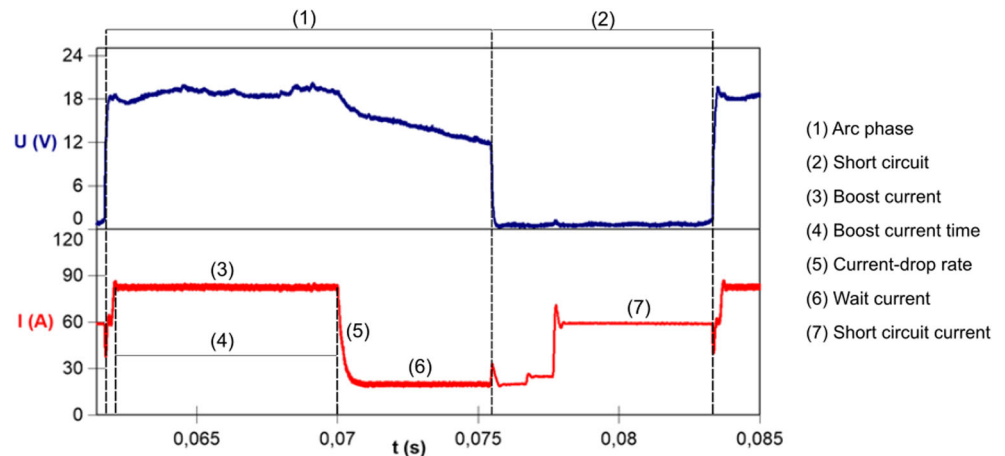
$$IV_{SC} = \frac{\sigma_{t_{sc}}}{t_{sc}} + \frac{\sigma_{t_{arcing}}}{t_{arcing}} \quad (1)$$

where

$\sigma_{t_{sc}}$  standard deviation of mean short-circuit time

$\sigma_{t_{arcing}}$  standard deviation of mean arc burning time

**Fig. 4** Fundamental parameters to determine CMT waveform



$t_{sc}$  short circuit mean time

$t_{arcing}$  arc burning time

As indicated above, the periods constancy is measured through the variation coefficient, which takes into account not only the standard deviation, but also the average. The lower the IV<sub>SC</sub>, the more regular is the metal transfer.

Considering the relevance of stability analysis in CMT MIGB process and the absence of studies in this field, the present paper aims to assess the influence of the current pulse (IBoost) parameter over metal transfer stability with the aid of a high-speed camera. Chen et al. [35] investigated the influence of IBoost over stability, varying it from 250 to 320 A during carbon steel welding and did not find a significantly alteration in the probability distribution of short-circuit periods. It is important to mention that this study was conducted in a welding process, and not in brazing. The objective here is to analyze the stability behavior of a brazing process based on IV<sub>SC</sub> and obtain bead uniformity, as well as favorable conditions for width and contact angle in ZnAl<sub>4</sub> deposits over a galvanized steel. The results are relevant to support the development of dissimilar materials brazing of aluminum and galvanized steel.

## 2 Methodology

### 2.1 Materials

The brazing process results were studied based on the analysis of the deposition of zinc alloy ZnAl<sub>4</sub> on the galvanized steel DX56D + Z140 (classified according to the German standard DIN EN 10346). The chemical composition of this alloy is in the range of 95.5 to 96.5% of zinc and 3.5 to 4.5% of aluminum.

The base material was selected because it is frequently applied in automotive manufacturing and presents high tension strength and processability when compared among other steels [22]. The samples had dimensions of 150 mm × 100 mm × 1 mm, while the filler material was in the wire format, with 1.2 mm diameter.



**Table 1** Selected CMT parameters for experiments

IBoost (A)	Vwf (m/min)	tBoost (ms)	Iwait (A)	Isc (A)	Idroprate (A/ms)
30	2.3	5.53	20	60	200
43	3.2	5.53	20	60	200
57	3.8	5.53	20	60	200
70	4.9	5.53	20	60	200
83	5.3	5.53	20	60	200
97	6.1	5.53	20	60	200
110	6.3	5.53	20	60	200
123	7.0	5.53	20	60	200
137	7.4	5.53	20	60	200
150	7.7	5.53	20	60	200

**2.2 Experimental procedure**

The experiments were carried out with a TransPuls Synergic 400 CMT™ power source and a RCU 5000 I interface integrated to a semi-mechanized welding system. It means that the torch was fixed by a mechanical support and the workpiece movement was executed with a linear axis table. The tests configuration is displayed in Fig. 3.

The brazing was carried out in the flat position with 0.35 m/min and 12 l/min of argon shielding (99.5%). The CMT wave can be divided in arc (1) and short circuit (2) phases, as indicated in Fig. 4. In addition, the fundamental parameters determining the waveform shape are boost current (3—IBoost), boost current time (4—tBoost), current drop rate (5—Idroprate), short-circuit wait current (6—Iw), and short-circuit current (7—Isc).

The IBoost current varied from 30 to 150 A and, consequently, the wire feed speed (Vwf), from 2.3 to 7.8 m/min. The remaining parameters were kept constant, as displayed in Table 1. As the study was based on tendencies, and not accuracy levels, just one test for each bead was carried out. When there is a small number of factors, as in this work (only IBoost current), the degree of freedom of the experiment is high enough. A consistent significance of the tendency can be reached if the hidden variance is low.

The transient electric signal acquisitions (current and voltage) were done with Yokogawa DL850E™ oscilloscope. The acquisition rate used was 200 kHz and the time for data

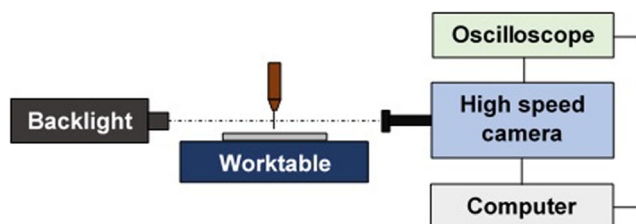


**Fig. 5** Configuration for image acquisition

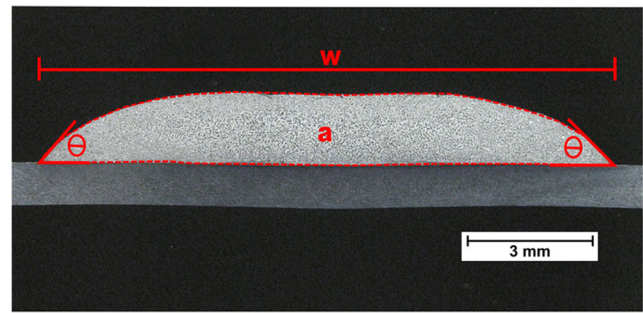


**Fig. 6** Example of wetting angle and length measurements from a bead cross-section

acquisition was 2 s, for all experiments. Simultaneously, the metal transfer was recorded by a Photron SA4™ high-speed camera with 200 kHz sampling frequency. The camera was aligned with the welding torch and a lamp. The camera software was connected to the oscilloscope and the trigger mode was activated aiming to obtain the images simultaneously with the electric signals. The configuration for image acquisition is illustrated schematically in Fig. 5. All the data (electric signals and high-speed records) were then processed in a computer, with special programs such as FlexPro® and LabVIEW™.

**2.3 Assessment of results**

The resultant bead in brazing should present good wettability. In order to assess this characteristic, cross-sections samples were taken and prepared for metallographic visualization, through sand gridding (from 80 to 1200 mesh), polishing (1 μm alumina), and etching (Nital 2%) procedures. The width (mm) and contact angle (°) were measured with a KEYENCE Digital Microscope VHX—500F, according to Fig. 6. The contact angle considered for correlation was obtained after calculation of the average between the left and the right angles of the sample. The image software ImageJ was

**Table 2** Measured width, contact angle, and cross-section area as a function of IBoost and wire feed speed (Vwf)

IBoost (A)	Vwf (m/min)	Width (mm)	Contact angle (°)	Area (mm <sup>2</sup> )
30	2.3	3.8	115	8.2
43	3.2	5.9	78	9.9
57	3.8	7.4	72	11.4
70	4.9	11.2	53	15.5
83	5.3	12.5	59	17.7
97	6.1	14.2	56	17.5
110	6.3	19.1	20	15.5
123	7.0	20.6	28	15.8
137	7.4	20.9	41	20.1
150	7.8	23.2	17	12.9

used for analysis. Low contact angle and long wetting width are positive indicators of wettability.

The influence of pulse current IBoost over process stability was first investigated based on current and voltage acquisition signals, with computation of arc burning and short-circuit times. Then, the IVsc could be calculated, according to Eq. (1). The premise for this index is that when arc burning and short-circuit times have low dispersion values, the heat transfer to the plate becomes stable, as well as the bead geometry and the metallurgical modifications. The periods constancy is measured through the variation coefficient, that takes into account not only the standard deviation, but also the average. The lower the IVsc, the more regular is the metal transfer.

The IVsc was correlated to the bead geometry (contact angle and width), and with captured images from high-speed videos.

### 3 Results and discussion

The bead width and contact angle are important factors for a brazed joint, as they can exert influence on the mechanical properties [12]. Table 2 shows the values for the measured width, contact angle, and cross-section area as a function of IBoost and wire feed speed (Vwf) after CMT brazing.

An increase in IBoost current from 30 to 150 A, and consequently, in Vwf from 2.3 to 7.8 m/min, led to an increase of width from 3.8 to 23.2 mm and a reduction of contact angle from 115 to 17°. The heat input has a direct relation with current. Therefore, this trend agrees with that presented by Basak et al. [10] in a pulsed MIGB.

The resultant macrographs are presented in Fig. 7. They can be classified in three groups. From 30 to 83 A, the beads had homogeneity, but the width and contact angle were not the most appropriate for brazing. When IBoost reached 97 A, the bead also presented homogeneity, with the maximum value

for width and the minimum for contact angle when compared among the samples from 30 to 83 A. After 97 A, the beads were not homogeneous anymore. The absence of homogeneity can be analyzed also based on the area values from Table 2. After 97 A, the cross-section area should have increased; however, this was not observed.

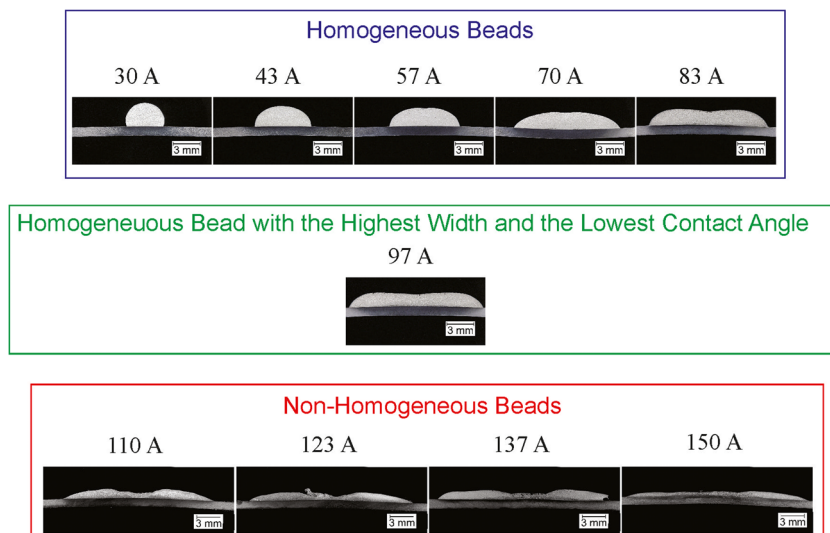
Figure 8 presents the relation for Vwf, IBoost, and width (a) as well as for Vwf, IBoost, and contact angle (b). It is important to note that high IBoost and Vwf values lead to high width and low contact angle, but it does not mean that the maximum width and minimum contact angle found are the best for brazing. The main reason is related to bead homogeneity. After 97 A, the beads were not uniform, so they cannot be applied industrially. The most suited IBoost is 97 A because it has homogeneity and simultaneously, the higher width and the lower contact angle when compared with the other homogeneous beads.

In order to understand the variation in homogeneity, a statistic analysis was conducted. For each IBoost value, the current and voltage oscillograms were acquired and the arc burning and short-circuit times were calculated for computation of IVsc, according to Eq. (1). The plot for IVsc as a function of IBoost is shown in Fig. 9.

In fact, the IVsc decreases from 30 to 97 A, and reaches the minimum value. At 97 A, the arc burning and short-circuit times present the lowest dispersion, which leads to homogeneous heat transfer to the plate, as well as uniform bead geometry and metallurgical alterations. After 97 A, the IVsc becomes high again, with reduced metal transfer stability.

The reason why the 97 A IBoost is the most appropriate parameter for brazing is clarified. However, it is important to note that samples from 30 to 57 A presented higher IVsc (lower metal transfer stability), than samples from 110 to 150 A, but did not fall in the non-homogeneous area.

**Fig. 7** Macrographs relative to IBoost variation from 30 to 150 A



In order to understand the phenomena, high-speed camera frames from Figs. 10 and 11 were analyzed. In Fig. 10, three IBoost levels were assessed: 30 A (a), 97 A (b), and 150 A (c) 1 ms after metal bridge detachment (beginning of arc burning time). Spattering is evident only for IBoost of 30 A. For 97 A and 150 A IBoost levels, arc burning behavior occurred as expected.

A similar analysis was conducted during metal bridge detachment, as shown in Fig. 11. Again, IBoost level of 30 A presented high degree of irregularity, while 97 A and 150 A showed a constant bridge size.

Therefore, IBoost level of 30 A presented an unstable metal transfer behavior, while for 97 A and 150 A levels, stability was reached. The bead homogeneity was found for IBoost

values below 97 A. This means that to determine homogeneity, the metal transfer stability, assessed through IVsc, is an indicator, but other factors must also be considered.

For 30 A, in spite of the absence of metal transfer stability, the low current level did not disturb the melt pool. For 97 A, the melt pool was not disturbed and it presented the best stability, according to IVsc value and high-speed camera frames. Finally, for 150 A, the metal transfer stability was also good, but homogeneity was not achieved due to melt pool disturbances. Disturbances are related to material behavior when faced with high temperature, such as metal vaporization and surface tension values. Melt pool convection can be significantly altered as a result of these factors. The IBoost current level of 97 A acted as a threshold, delimitating homogeneous

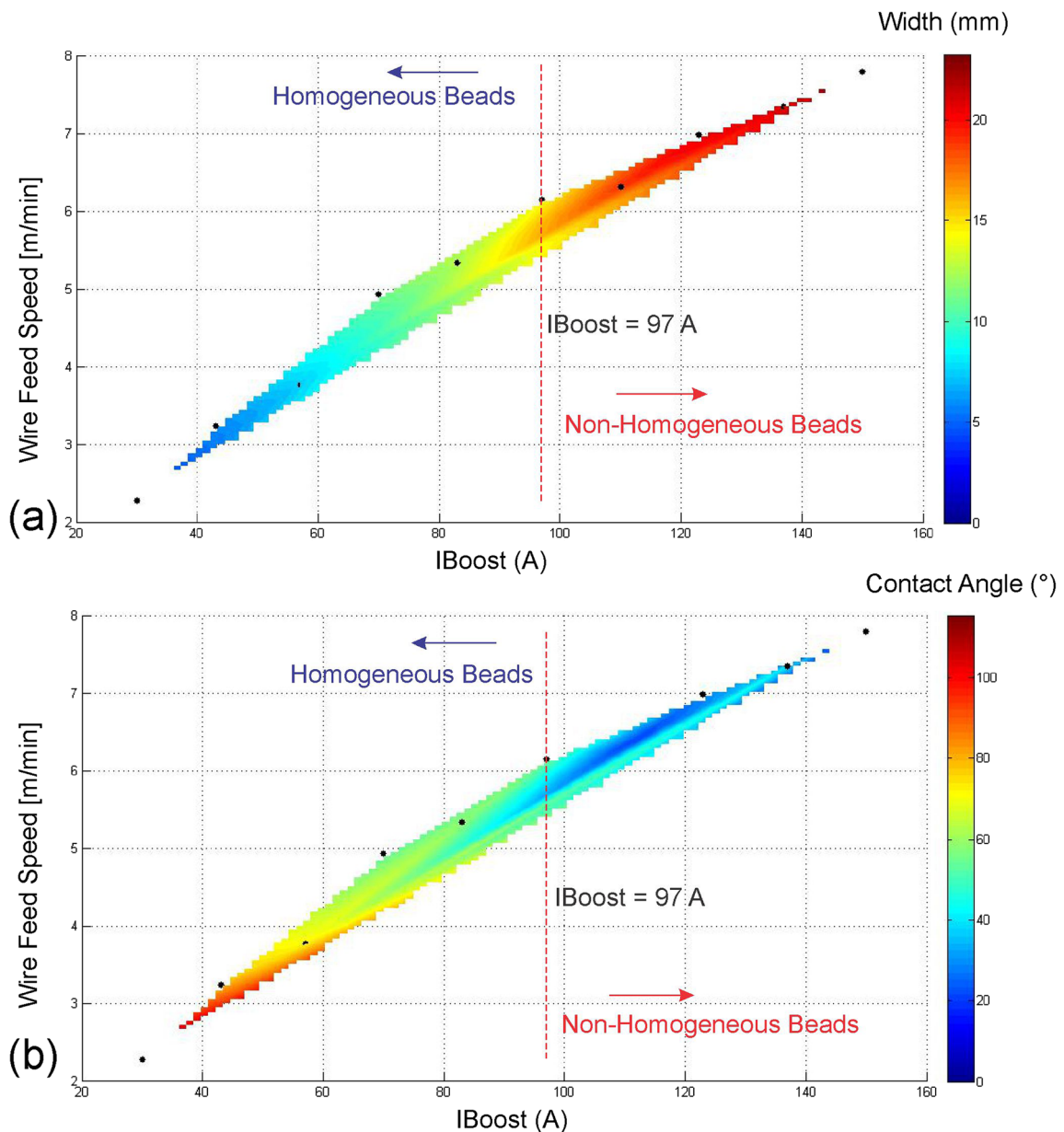
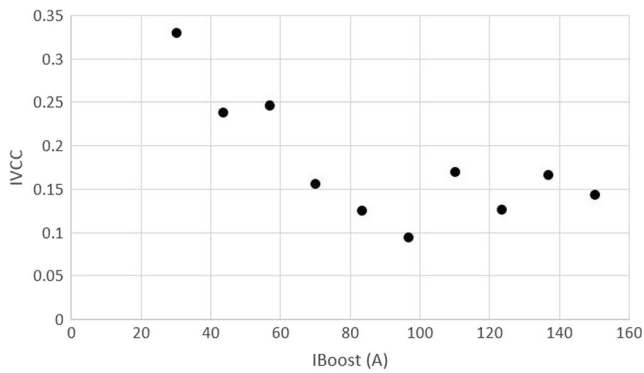


Fig. 8 a Relation between wire feed speed (Vwf), IBoost, and bead width. b Relation between wire feed speed (Vwf), IBoost, and bead contact angle



**Fig. 9** Relation between IVsc and IBoost

beads from non-homogeneous ones, and was more relevant than the metal transfer stability.

The influence of IBoost on metal transfer was previously studied by Chen et al. [35] after varying it from 250 to 320 A during carbon steel welding. Nevertheless, they did not find a correlation between IBoost variation and metal transfer stability, which differs from this work. Two factors may have contributed to that. The first one is the analyzed range of 250 to 320 A, which is narrow and insufficient to scan stability behavior. The second is related to the materials involved that show completely different behavior when subjected to current flow and arc voltage.

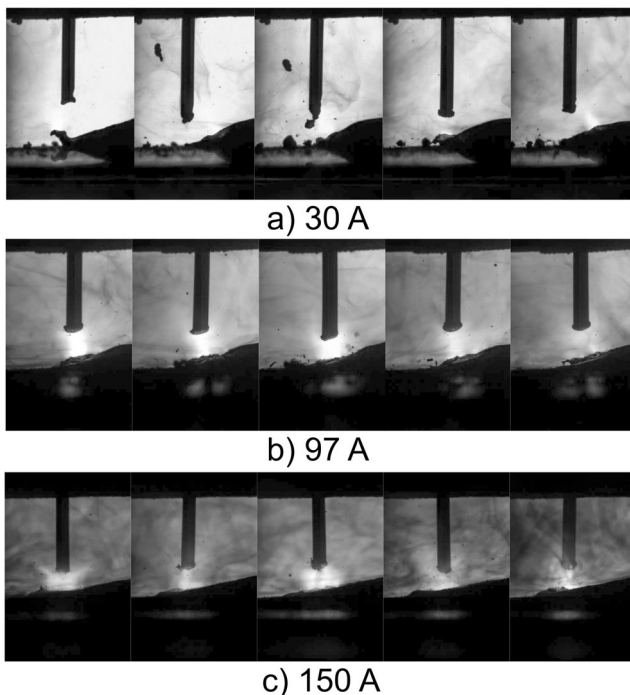


**Fig. 10** Metal transfer behavior for IBoost of 30 A (a), 97 A (b), and 150 A (c), 1 ms after metal bridge detachment (beginning of arc burning time)

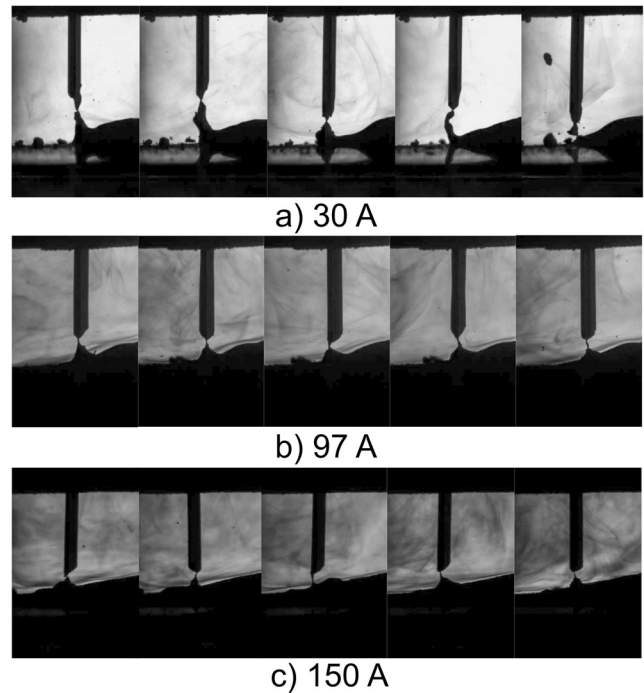


**Fig. 11** Metal transfer behavior for IBoost of 30 A (a), 97 A (b), and 150 A (c), during metal bridge detachment

## 4 Conclusion

The stability behavior of the CMT brazing investigated in this paper is a function of IBoost current. The statistical index IVsc, which can be correlated to metal transfer stability, decreased for the range of IBoost current from 30 to 97 A, reached the minimum value at 97 A, and became high again until 150 A. The lower the IVsc, the more stable is the process. Then, when IBoost was set to 97 A, the process reached the higher stability level.

The analysis of high-speed camera results for IBoost current of 30 A, 97 A, and 150 A pointed that only in 30 A the metal transfer presented significant level of spatters and irregularities, while in 97 A and 150 A showed a repetitive behavior, without spatters.

The bead homogeneity did not follow the same trend of stability. The bead homogeneity was found for IBoost values below 97 A. From 110 to 150 A, non-homogeneous beads were formed, in spite of the good stability verified for 150 A with high-speed images. This means that to determine homogeneity, the metal transfer stability, assessed through IVsc, is an indicator, but other factors must also be considered. High current levels can lead to melt pool disturbances. These disturbances are related to material behavior when faced with high temperature, such as metal vaporization and surface tension values. Melt pool convection can be significantly altered as a result of these factors.

The IBoost current, and consequently, the heat input, could be correlated to bead dimensions. An increase in IBoost



current from 30 to 150 A led to and increase of width from 3.8 to 23.2 mm, and a reduction of contact angle from 115 to 17°. However, after 97 A, the beads were not uniform, so they cannot be applied industrially. The most suited IBoost is 97 A because it has homogeneity and simultaneously, the higher width and the lower contact angle when compared with the other homogeneous beads. These results are relevant to support the development of dissimilar materials brazing of aluminum and galvanized steel.

## References

- Ünel E, Taban E (2017) Properties and optimization of dissimilar aluminum steel CMT welds. *Weld World* 61:1–9. <https://doi.org/10.1007/s40194-016-0386-9>
- Sun J, Huang J, Yan Q, Li Z (2016) Fiber laser butt joining of aluminum to steel using welding-brazing method. *Int J Adv Manuf Technol* 85:2639–2650. <https://doi.org/10.1007/s00170-015-8137-4>
- Kang M, Kim C (2015) Joining Al 5052 alloy to aluminized steel sheet using cold metal transfer process. *J Mater* 81:95–103. <https://doi.org/10.1016/j.matdes.2015.05.035>
- Basak S, Pal TK, Shome M (2016) High-cycle fatigue behavior of MIG brazed galvanized DP600 steel sheet joint—effect of process parameters. *Int J Adv Manuf Technol* 82:1197–1211. <https://doi.org/10.1007/s00170-015-7451-1>
- Acarer M, Demir B (2008) An investigation of mechanical and metallurgical properties of explosive welded aluminum—dual phase steel. *Mater Lett* 62:4158–4160. <https://doi.org/10.1016/j.matlet.2008.05.060>
- Murray RT (2007) The behaviour of iron and aluminium during the diffusion welding of carbon steel to aluminium. *J Mater Sci* 42: 5692–5699. <https://doi.org/10.1007/s10853-006-0742-z>
- Handa A, Chawla V (2014) Investigation of mechanical properties of friction-welded AISI 304 with AISI 1021 dissimilar steels. *Int J Adv Manuf Technol* 75:1493–1500. <https://doi.org/10.1007/s00170-014-6238-0>
- Watanabe T, Takayama H, Yanagisawa A (2006) Joining of aluminum alloy to steel by friction stir welding. *J Mater Process Technol* 178:342–349. <https://doi.org/10.1016/j.jmatprotec.2006.04.117>
- Li J, Li H, Huang C, Xiang T, Ni Y, Wei H (2017) Welding process characteristics of pulse on pulse MIG arc brazing of aluminum alloy to stainless steel. *Int J Adv Manuf Technol* 91:1057–1067. <https://doi.org/10.1007/s00170-016-9820-9>
- Basak S, Das H, Kumar T, Shome M (2016) Characterization of intermetallics in aluminum to zinc coated interstitial free steel joining by pulsed MIG brazing for automotive application. *Mater Charact* 112:229–237. <https://doi.org/10.1016/j.matchar.2015.12.030>
- Li J, Li H, Wei H, Gao Y (2016) Effect of torch position and angle on welding quality and welding process stability in Pulse on Pulse MIG welding—brazing of aluminum alloy to stainless steel. *Int J Adv Manuf Technol* 84:705–716. <https://doi.org/10.1007/s00170-015-7734-6>
- Jenney CL, O'Brien A (1991) *Welding handbook*. Am Weld Soc <https://doi.org/10.1017/CBO9781107415324.004>
- Mathieu A, Shabadi R, Deschamps A, Suery M, Mattei S, Grevey D, Cicala E (2007) Dissimilar material joining using laser aluminum to steel using zinc-based filler wire. *Opt Laser Technol* 39: 652–661. <https://doi.org/10.1016/j.optlastec.2005.08.014>
- Cao R, Chang JH, Huang Q, Zhang XB, Yan YJ, Chen JH (2018) Behaviors and effects of Zn coating on welding-brazing process of Al-Steel and Mg-steel dissimilar metals. *J Manuf Process* 31:674–688. <https://doi.org/10.1016/j.jmapro.2018.01.001>
- Dharmendra C, Rao KP, Wilden J, Reich S (2011) Study on laser welding—brazing of zinc coated steel to aluminum alloy with a zinc based filler. *Mater Sci Eng A* 528:1497–1503. <https://doi.org/10.1016/j.msea.2010.10.050>
- Alloy AZ, Steel G, Lin Q et al (2015) Wetting and interfacial characteristics cold metal transfer process. *Metall Mater Trans A* 46: 3793–3796. <https://doi.org/10.1007/s11661-015-3005-2>
- Ahsan et al. (2016) Cold Metal Transfer (CMT) GMAW of zinc—coated steel. *Weld J* 95:120–132
- Wilden J, Bergmann JP, Dolles M, Reich S (2005) Use of zinc-alloys for low temperature soldering of zinc coated steels. *Adv Mater Res* 8:127–134. <https://doi.org/10.4028/www.scientific.net/AMR.6-8.127>
- Mohammadpour M, Yazdian N, Wang H et al (2018) Effect of filler wire composition on performance of Al/Galvanized steel joints by twin spot laser welding-brazing method. *J Manuf Process* 31:20–34. <https://doi.org/10.1016/j.jmapro.2017.11.007>
- Taban E, Gould JE, Lippold JC (2010) Characterization of 6061-T6 aluminum alloy to AISI 1018 steel interfaces during joining and thermo-mechanical conditioning. *Mater Sci Eng A* 527:1704–1708. <https://doi.org/10.1016/j.msea.2009.10.059>
- Lee W, Schmuecker M, Mercardo A et al (2006) Interfacial reaction in steel—aluminum joints made by friction stir welding. *Scr Mater* 55:355–358. <https://doi.org/10.1016/j.scriptamat.2006.04.028>
- Lee K, Kumai S, Kawamura N et al (2007) Growth manner of intermetallic compounds at the weld interface of steel/aluminum alloy lap joint fabricated by a defocused laser beam. *Mater Trans* 48: 1396–1405. <https://doi.org/10.2320/matertrans.L-MRA2007838>
- Lee K, Kumai S (2006) Characterization of intermetallic compound layer formed at the weld interface of the defocused laser welded low carbon steel/6111 aluminum alloy lap joint. *Mater Trans* 47:1178–1185
- Murakami T, Nakata K, Tong H, Ushio M (2003) Dissimilar metal joining of aluminum to steel by MIG arc brazing using flux cored wire. *ISIJ International* 43:1596–1602
- Milani AM, Paidar M, Khodabandeh A, Nategh S (2016) Influence of filler wire and wire feed speed on metallurgical and mechanical properties of MIG welding—brazing of automotive galvanized steel/5754 aluminum alloy in a lap joint configuration. *Int J Adv Manuf Technol* 82:1495–1506. <https://doi.org/10.1007/s00170-015-7505-4>
- Zhang HT, Feng JC, He P, Zhang BB, Chen JM, Wang L (2009) The arc characteristics and metal transfer behaviour of cold metal transfer and its use in joining aluminium to zinc-coated steel. *Mater Sci Eng A* 499:111–113. <https://doi.org/10.1016/j.msea.2007.11.124>
- Angerhausen M, Geffers C, Reisgen U, Willms K, Hof S, Prenger F, Deckert K (2014) Thermal joining with zinc based solder—new potentials for structural lightweight design. *Mater Sci Forum* 786: 2741–2746. <https://doi.org/10.4028/www.scientific.net/MSF.783-786.2741>
- Dutra JC, Henrique R, Savi BM (2015) Metallurgical characterization of the 5083H116 aluminum alloy welded with the cold metal transfer process and two different wire-electrodes (5183 and 5087). *Weld World* 59:797–807. <https://doi.org/10.1007/s40194-015-0253-0>
- Kah P, Suoranta R, Martikainen J (2013) Advanced gas metal arc welding processes. *Int J Adv Manuf Technol* 67:655–674. <https://doi.org/10.1007/s00170-012-4513-5>
- Mei SW, Gao M, Yan J, Zhang C, Li G, Zeng XY (2013) Interface properties and thermodynamic analysis of laser—arc hybrid welded

- Al/steel joint. *Sci Technol Weld Join* 18:293–301. <https://doi.org/10.1179/1362171813Y.0000000106>
31. Elrefaey A (2015) Effectiveness of cold metal transfer process for welding 7075 aluminium alloys. *Sci Technol Weld Join* 20:280–286. <https://doi.org/10.1179/1362171815Y.0000000017>
  32. Li BJ, Sun Q, Liu Y et al (2016) Cold metal transfer welding—brazing of pure titanium TA2 to aluminum alloy 6061-T6 \*\*. *Adv Eng Mater* 19:1–8. <https://doi.org/10.1002/adem.201600494>
  33. Cao R, Zhu HX, Wang Q, Dong C, Lin Q, Chen JH (2016) Effects of zinc coating on magnesium alloy—steel joints produced by cold metal transfer method. *Mater Sci Technol* 32:1805–1817. <https://doi.org/10.1080/02670836.2016.1148107>
  34. Alves V, Meneses D, Fernando J et al (2014) *Journal of Materials Processing Technology* The effect of metal transfer stability (spattering) on fume generation, morphology and composition in short-circuit MAG welding. *J Mater Process Technol* 214:1388–1397. <https://doi.org/10.1016/j.jmatprotec.2014.02.012>
  35. Chen M, Zhang D, Wu C (2017) *Journal of Materials Processing Technology* Current waveform effects on CMT welding of mild steel. *J Mater Process Technol* 243:395–404. <https://doi.org/10.1016/j.jmatprotec.2017.01.004>

**Publisher's note** Springer Nature remains neutral with regard to jurisdictional claims in published maps and institutional affiliations.